Heat-induced transposition leads to rapid drought resistance of *Arabidopsis thaliana*

Michael Thieme[1]*, Arthur Brêchet[2], Yann Bourgeois[3], Bettina Keller[1], Etienne Bucher[4] and Anne Roulin[1]

1 Department of Plant and Microbial Biology, University of Zürich, Zollikerstrasse 107, 8008 Zürich, Switzerland

2 Botanical Institute, Zürich-Basel Plant Science Center, University of Basel, Hebelstrasse 1, 4056 Basel, Switzerland

3 School of Biological Sciences, University of Portsmouth, PO1 2DT Portsmouth

4 Plant Breeding and Genetic Resources, Agroscope, 1260 Nyon, Switzerland

* author for correspondence: michael.thieme@botinst.uzh.ch

Abstract

Plant genomes comprise a vast diversity of transposable elements (TEs) (Tenaillon et al. 2010). While their uncontrolled proliferation can have fatal consequences for their host, there is strong evidence for their importance in fueling genetic diversity and plant evolution (Baduel et al. 2021). However, the number of studies addressing the role of TEs in this process is limited. Here we show that the heat-induced burst of a low-copy TE increases phenotypic diversity and leads to the rapid emergence of more drought-resistant individuals of *Arabidopsis thaliana*. We exposed TE-high-copy-(hc)lines (Thieme et al. 2017) with up to ~8 fold increased copy numbers of the heat-responsive *ONSEN*-TE (*At*COPIA78) (Ito et al. 2011; Cavrak et al. 2014; Tittel-Elmer et al. 2010) in the wild type background to desiccation as a straightforward and highly relevant selection pressure. We found evidence for a drastic increase of drought resistance in five out of the 23 tested hc-lines and further pinpoint one of the causative mutations to an exonic *ONSEN*-insertion in the *ribose-5-phosphate-isomerase 2* gene. This loss-of-function mutation resulted in a decreased rate of photosynthesis and water consumption. This is one of the rare examples (Esnault et al. 2019) experimentally demonstrating the adaptive potential of mobilized stress-responsive TEs in eukaryotes. Our results further shed light on the complex relationship between mobile elements and their hosts and substantiate the importance of TE-mediated loss-of-function mutations in stress adaptation, particularly with respect to global warming.

Keywords: *Arabidopsis thaliana*, *ONSEN,* transposable element, adaptation, evolution, loss-of-function mutation, drought stress, climate change

Introduction

Plants are constantly exposed to fluctuating environments. To successfully reproduce, they thus rely on mechanisms that allow them to react and adapt to suboptimal growth conditions. Water limitation caused by increased evaporation or decreased precipitation is one of the major constraints impacting fitness and distribution of plants and among them crops (Gupta et al. 2020). Due to climate change, drought is expected to constitute a severe environmental constraint to which plants will have to adapt in a near future (Dai 2013; FAO 2019). Genetic variation, whether as a result of natural processes or artificially induced, is a prerequisite for adaptation and the evolution of new traits. An increasing body of evidence suggests that the rate of natural mutations not only depends on the genomic context (Weng et al. 2019) but can also be altered by severe environmental stresses such as heat (Lu et al. 2021; Belfield et al. 2021). Besides single nucleotide polymorphisms and small insertions or deletions, external triggers also affect genome integrity through the stress-induced activation of transposable elements (TEs) (Negi et al. 2016). TEs are mobile DNA sequences that are especially abundant in plant genomes (Tenaillon et al. 2010) and highly mutagenic. Indeed, TEs can not only efficiently knock out genes (Ram et al. 2019) but also bring their flanking regions under epigenetic control or render them stress responsive (Grandbastien 2015; Makarevitch et al. 2015; Roquis et al. 2021; Ito et al. 2011; Butelli et al. 2012). By proliferating in response to the environment, stress-inducible TEs are thus believed to be prone to produce the raw material necessary for individuals to respond to challenging environments (Baduel et al. 2021; Li et al. 2018). Yet, despite reports about TE bursts (Piegu et al. 2006; Naito et al. 2009), transposon amplification is rather a gradual process that happens over many generations (Stritt et al. 2018). Indeed, TE-mobility in plants is usually restricted by epigenetic silencing mechanisms including RNA-directed DNA-methylation (RdDM) that ensures a limited mutation rate to safeguard genome stability (Matzke and Mosher 2014). As a consequence, and despite an increasing number of examples highlighting how TEs may shape phenotypes and be positively selected in natural systems and crops (e.g. Lisch 2013; Bourgeois and Boissinot 2019), real-time observations assessing the evolutionary consequences of stress-induced TE mobilisations are rare. In this context, we study here the functional impact of the *Arabidopsis thaliana* retrotransposon *ONSEN* (*At*COPIA78), one of the best characterized TE-families in plants. Equipped with heat-responsive elements in its Long-Terminal Repeats (LTRs), *ONSEN* can sense the heat-stress-response of its host and utilize it to initiate its own lifecycle (Tittel-Elmer et al. 2010; Ito et al. 2011; Cavrak et al. 2014). In the *A. thaliana* ecotype Col-0 that usually carries eight full-length copies in its genome, we have previously shown that the chemical inhibition of DNA-methyltransferases and RNA-polymerase II in combination with a heat shock leads to the transpositional activity of *ONSEN* in wild type (wt) plants. This experiment resulted in the

establishment of genetically stable high-copy (hc)-lines, some of which displaying more than eight-fold increased *ONSEN* copy numbers (Thieme et al. 2017). Here, we used 23 of the these *ONSEN* hc-lines to characterize how stress-inducible TEs contribute to phenotypic plasticity and stress resilience in *A. thaliana*. To do so, we deployed the machine learning algorithm ilastik (Berg et al. 2019) for a image-based assessment of drought resistance among the hc-lines. We show that the heat-induced transposition of *ONSEN* resulted in the frequent emergence of drought-resistant individuals. By further characterizing the most drought resistant hc-line, we determined that the vitality of this line was enhanced by an *ONSEN*-mediated loss-of-function (LoF) mutation of the *ribose-5-phosphate-isomerase 2* (*RPI2*). Our study does not only highlight how fast TEs may mediate large-effect mutations and adaptation but also shows that LoF alleles can play an important role in this process.

Results

ONSEN hc-lines differ in growth

To determine the evolutionary potential of the heat-induced transposition of *ONSEN*, we grew the S4 generation of 23 hc-lines originating from 13 independent heat stressed and transiently de-methylated plants (Thieme et al. 2017) with up to ~8 fold increased copy numbers, thus up to ~64 stably inserted *ONSEN* copies (Fig 1a) under highly controlled conditions. Notably, due to the sensitivity of the qPCR we could not detect additional *ONSEN* copies in hc-lines with only few additional *ONSEN* insertions. The presence of novel *ONSEN* copies for instance in hc9 (plus one homozygous and two heterozygous copies compared to wt) has however been shown previously by sequencing (Roquis et al. 2021). As the hc-lines were originally exposed to a combination of heat and the drugs zebularine (Z) and alpha-amanitin (A) (HS+AZ) (Thieme et al. 2017; Baubec et al. 2009), we controlled for a potential *ONSEN*-independent phenotypic variation caused by epi/genetic changes induced by the heat-stress or the chemical demethylation. To do so, we included a Col-0 wt that was propagated on soil and five independent controls, i.e. lines that originated from plants that were also grown *in vitro* but only exposed to control-stress (CS; two lines), heat-stress (HS; two lines) or CS plus chemical demethylation (CS+AZ; one line) (Thieme et al. 2017). In accordance with previous observations (Thieme et al. 2017; Roquis et al. 2021), we did not detect an increase in *ONSEN* copy numbers in these control lines when compared to the wt (Fig 1a).

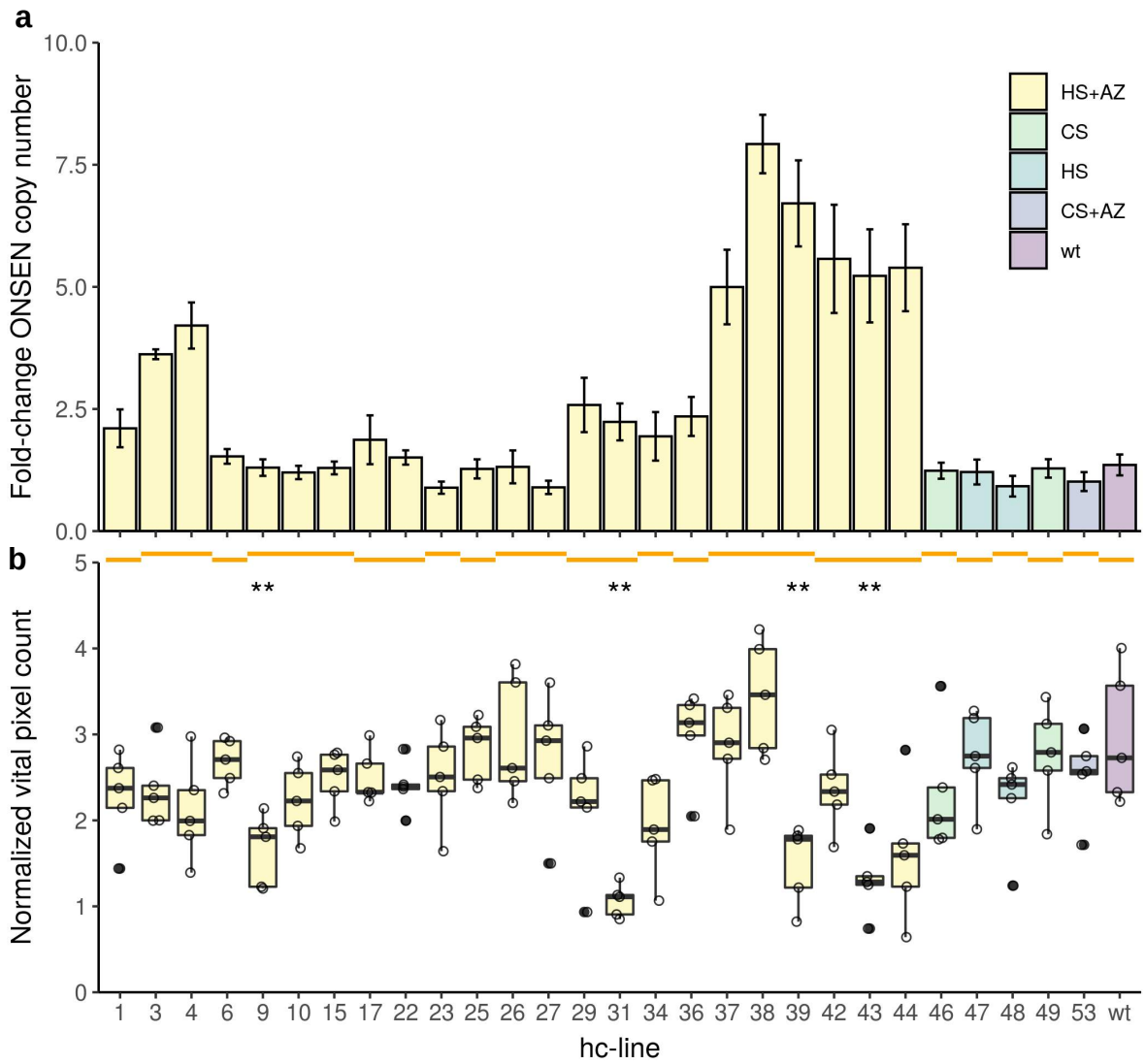

Fig. 1 ***ONSEN* copy numbers and size of hc-lines.** Colors of boxes indicate the history of lines: control-stress (CS), heat-stress (HS), chemical de-methylation (AZ) and Col-0-wild type propagated on soil (wt). Continuous orange lines spanning multiple hc-lines indicate their origin from a common parent. **a** Fold-change of *ONSEN* copy numbers measured by qPCR compared to the wt (n=3 technical replicates +/- SD). **b** Vital pixel count of hc-lines and controls before the occurrence of wilted leaves (day 8). Significant differences to the wt are indicated. n= 5 biological replicates. Wilcoxon-test P< 0.01 (**).

After 36 days of growth under short day conditions, we suspended watering and recorded plant growth and water loss of the pots every week by taking top view pictures and by weighting the pots. To quantify the growth and degree of drought-induced wilting of leaves, we trained the machine learning software ilastik (Berg et al. 2019) to specifically detect vital and dead segments of leaves. We first tested the reliability of the prediction by placing one to three punched leaf-discs of wilted or green segments onto a pot that did not contain a plant. After processing the images with ilastik, we obtained a linear increase of green and wilted pixel-counts according to the number of segments placed onto the pots (Fig S1), confirming the reliability of the method. For the rest of the study, we therefore use vital pixel counts as a proxy for plant size. To assess size variations between the hc-lines, we analyzed the pixel counts of predicted green areas before the appearance of wilted leaves eight days after watering was suspended (Fig 1b, Fig 2a). While the five controls did not differ from the wt, we found a great size variation between lines with four hc-lines showing a significantly reduced number of green pixels compared to the wt (Wilcoxon-test $P<0.01$). Notably, in some cases we also observed a strong size variation between hc-lines originating from the same parent (e.g. hc37 and hc38 vs hc39) indicating genetic segregation of the lines (Fig 1b). We did not find any significant correlation between global *ONSEN*-copy numbers and plant size ($P>0.05$, Fig S2).

ONSEN hc-lines differ in drought resistance

The machine learning approach allowed us to track the dynamics of growth and drought-induced wilting of the individual hc-lines. Until 15 days after watering was suspended, none of the plants showed obvious signs of wilting (Fig 2a). Further desiccation of the pots resulted in the occurrence of wilted leaves in most of the lines, indicating that they were exposed to severe water-limitation. After 27 days, we resumed watering and recorded leaf areas after two days of recovery (day 29). In contrast to the high drought-induced mortality of the five control lines and the wt, we found that five out of the 23 hc-lines originating from four independent parental lines were more stress-resilient (mean vital leaf area > 50%) (Fig 2b). Notably, while the wt was most susceptible to desiccation (0.03 % mean vital area), hc31 the line displaying the highest resistance did not show any signs of wilting (97.9 % mean vital area, Fig 2a, b and c). The consistent vitality of all five replicates of hc31 pointed towards a homozygous mutation underlying the observed drought-resilience of this line. Because of this clear phenotype, hc31 was a prime candidate to characterize the functional link between the heat-induced insertion of novel *ONSEN* copies and the observed increase in drought resistance.

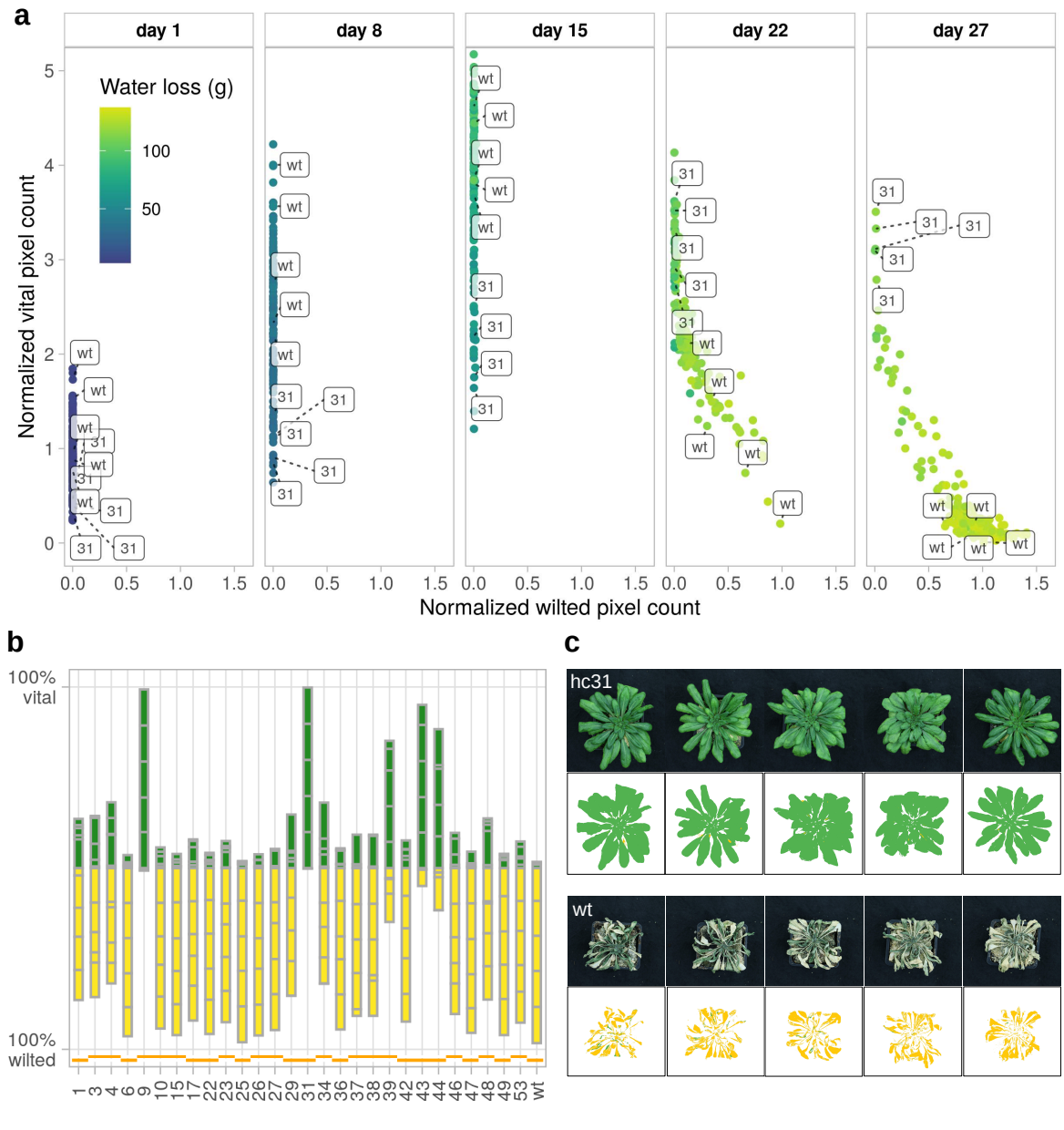

Fig. 2 **Drought resistance of *ONSEN* hc-lines. a** Development of vital and wilted pixel counts during the drought-stress. Each dot represents one individual plant and the color code indicates the cumulative water loss over time. n=3-5 biological replicates per line. **b** Sum of vital (green) and wilted (yellow) pixel counts of all five replicates per line two days after recovery (day 29). The contribution of each replicate to the total amount of vital and wilted pixels is indicated with gray bars. Continuous orange lines spanning multiple hc-lines indicate their origin from a common parent. **c** Original (top) and processed (ilastik, bottom) images of the five replicates of hc31 (top) and wt (bottom) on day 29. Predicted vital leaf segments are depicted in green, wilted ones in yellow.

An *ONSEN*-mediated loss-of-function causes increased drought resistance of hc31

First, we used whole-genome re-sequencing data to locate all transposon-insertion polymorphisms (TIPs) of hc31 (Roquis et al. 2021). Out of the ten *ONSEN*-TIPs detected in hc31, six were located in exons (Table 1). Notably, we detected a homozygous TIP in *RPI2* (*At*2G01290), a cytosolic ribose-5 phosphate isomerase that has previously been shown to play a role in chloroplast photosynthetic capacity (Xiong et al. 2009).

chr	*coordinates*	**context**	*ID*	*description*	*zygosity*
1	21761950– 55	exon	AT1G58602	LRR and NB-ARC domains-containing disease resistance protein	(-/-)
2	149387- 91	exon	AT2G01290	cytosolic ribose-5-phosphate isomerase	(-/-)
3	19300993– 97	exon	AT3G52020	serine carboxypeptidase-like 39	(+/-)
3	22631755- 59	exon	AT3G61150	homeodomain GLABROUS 1; HD-ZIP IV family.	(+/-)
5	853776- 80	exon	AT5G03435	Ca2+dependent plant phosphoribosyltransferase family protein	(-/-)
5	10632816– 20	TE	AT5G28626	AT5TE38720; SADHU; Sadhu non-coding retroTE family	(-/-)
5	18850327- 31	promoter	AT5G46490	disease resistance protein (TIR-NBS-LRR class) family	(-/-)
5	21050239- 43	intron	AT5G51800	protein kinase superfamily protein	(-/-)
5	21602030- 34	exon	AT5G53240	hypothetical protein (DUF295)	(+/-)
5	22846432- 36	intron	AT5G56400	FBD, F-box, Skp2-like and Leucine Rich Repeat domains containing protein	(+/-)

Table 1 **Novel *ONSEN* insertions in hc31**. Location, description (Araport11) and zygosity (-/- homo *ONSEN*, +/- hetero) of predicted *ONSEN* insertion sites according to Roquis et al. 2021.

We hypothesized that the exonic insertion of *ONSEN* in *RPI2* led to a LoF allele in hc31. The analysis of previously published RNA-seq data of hc31 (Roquis et al. 2021) indeed revealed a premature transcriptional stop coinciding with the detected exonic *ONSEN*-insertion in *RPI2* (Fig 3a). To test whether the knock-out of *RPI2* by *ONSEN* was causative for the observed high survival rate of hc31, we used the *rpi2-1* mutant (SALK_022117) (Xiong et al. 2009) that harbored a homozygous T-DNA insertion in the exon of *RPI2*. We crossed hc31 to the wt and the *rpi2-1*-mutant (Fig 3b) and recorded the drought resistance of the segregating F2-generations obtained from self-fertilization. We found that all individuals that were either homozygous for the *ONSEN*- or the T-DNA-insertion or that carried both the *ONSEN* and the T-DNA-insertions in *RPI2* survived the drought stress and showed an increase of vital area two days after recovery from drought stress. In contrast, plants that carried at least one wt allele showed a high degree of wilting and no increase of vital area two days after recovery from drought stress (Fig 3c,d). Altogether, these results confirmed that the insertion of *ONSEN* in *RPI2* mediates a recessive LoF mutation and causes the drought resistance of hc31.

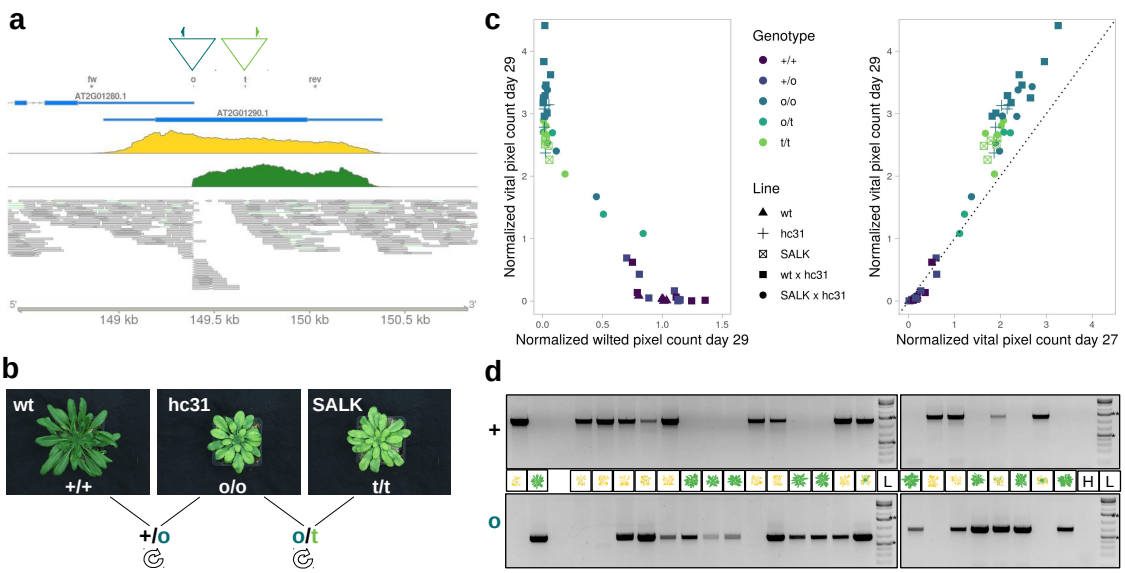

Fig. 3 **An *ONSEN*- insertion in *RPI2* leads to an increased drought resistance of hc31. a** Triangles indicate the insertion site of *ONSEN* (turquoise) and the location of the T-DNA in SALK_022117 (green) on chromosome 2. Primer locations used for the genotyping in **c** and **d** are depicted as filled triangles. Annotation track (blue), RNA-seq coverage of the wt (yellow) and hc31 (green) and aligned genomic reads from hc31 are shown. **b** Images and crossing scheme of the wt, hc31 and SALK_022117. Genotypes are depicted with + (wt), o (*ONSEN*), t (T-DNA). **c** Vital pixel counts after two days of recovery (day 29) in relation to wilted pixel counts on the same day (left panel) and compared to vital pixel counts before recovery (day 27) (right panel). Shapes indicate line (parental or segregating F2 generation of the crosses from **b**) and colors the genotype of *RPI2*. **d** Geno- and phenotypes (day 29) of the segregating F2 population of hc31 x wt. Two parental plants (wt and hc31, first two lanes) are shown. Primers specific for the wt (top gel, +) and the *ONSEN*- insertion (bottom gel, o) (see **a**) were used. H= water control, L=GeneRuler 1kb Plus ladder. 0.5 kb (*) and 1.5 kb (**) bands are marked.

Reduced water use leads to drought escape of hc31

Because of previous work indicating that the loss of *RPI2* leads to chloroplast dysfunction (Xiong et al. 2009), we further tested whether a reduction in the photosynthesis rate was associated to the observed drought resistance of hc31. Hence, we assessed the SPAD-values and carbon/nitrogen (C/N)-ratios following growth under well-watered conditions as those two variables can be directly linked to photosynthetic activity (Ling et al. 2011; Otori et al. 2017). We found in both cases a significant (Wilcoxon-test, $P<0.05$) reduction in hc31 compared to the wt (Fig 4a). Because we noted that before the onset of a severe water-limitation hc31 was significantly smaller compared to the wt (Fig 2a), we tested for a general link between plant size and drought resistance. We first fitted a linear model where water loss (before the occurrence of wilted leaves until day8 of the experiment) was entered as the response variable and the lines, vital pixel count and their interaction as explanatory

variables. While the overall model was significant and explained a large part of the variance (R^2 =0.72, P < 2.2e-16) we did not detect a significant contribution of line or the interaction of line and vital pixel count, indicating that all the hc-lines and wt harbored a similar efficiency regarding water use. However, we found that vital pixel count had a significant effect on water loss (P = 5.19e-11). This was further confirmed by a reduced model where the line and interaction effects were dropped (Fig 4b, R^2 0.71, P<0.001).

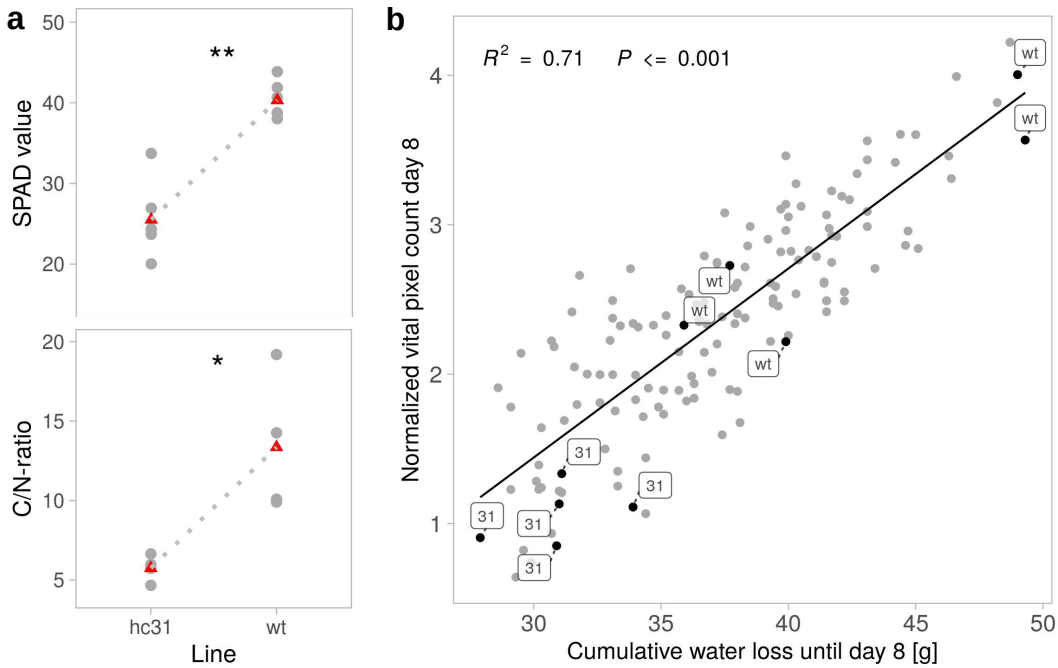

Fig. 4 **Physiological differences between hc31 and the wt.**
a SPAD meter values (top) and C/N-ratio (bottom) of the two lines. n= 4-6 biological replicates. Mean is marked with red triangle, Wilcoxon-test P<0.05 (*) 0.01 (**). **b** Relationship between vital pixel count and cumulative water loss until day 8 before the occurrence of wilted pixels. Linear regression model, adjusted R-squared: 0.71. P<0.001.

RPI2 variants in natural population are associated with aridity

We further tested the link between *RPI2* and resistance to aridity by selecting 596 genetically distinct *A. thaliana* ecotypes (kinship coefficient <0.5 and no missing data for subsequent analyses) from the 1001 genome project (Alonso-Blanco et al. 2016, Table S1). Global Aridity Index in summer (GAI_{summer}; Global Aridity Index averaged over April to August) extracted at each ecotype locality was significantly correlated with maximal temperature, solar radiation or precipitation levels (Fig S3a), and was thus used as a summary bioclimatic variable. We identified eleven SNPs with a maf > 0.3 in *RPI2*. While some of these SNPs are in strong linkage disequilibrium (Fig S3b), one of them located in the regulatory region of *RPI2* (chr2 at nt150495) showed a stronger association with GAI_{summer} (Fig S3b,c). Our linear-mixed model analysis showed that this SNP is significantly associated with higher GAI_{summer} even when accounting for population structure (Fig S3d) and suggested that *RPI2* plays a quantitative role (4.3% of the variance explained; Fig S3d) in the adaptation to arid climate in *A. thaliana* natural populations.

Survival probability of *ONSEN* in *RPI2*

We did not find any naturally occurring TIPs in *RPI2* (Baduel et al. 2021). This suggested that negative selection acts on TE-insertions in *RPI2* in natural populations. We used simulations to determine if and under which conditions large-scale mutations with strong phenotypic effects could reach high frequency in *A. thaliana* populations undergoing temporary drought stress (Fig S4). Four parameters were applied to control the simulations: the number of drought events (one to four), the length of each drought event (two to four generations) and the selective advantage of the insertion during drought (s+) and normal conditions (s-). We used a model of “hard” selection, where the population size varies as a function of the average fitness. When drought events were rare and short, no TIP was found in the population after 50 generations. However, the frequency of the TIP increased with higher values of s+ and lower values of s-, but required frequent and long episodes of drought events.

Discussion

In the context of climate change, assessing how fast plants will adapt to longer periods of severe heat and drought-stress is crucial both for conservation biology and food security (Brás et al. 2021; Loarie et al. 2009; Exposito-Alonso et al. 2019). Selection from standing variation, as opposed to the emergence of new mutations (Hermisson and Pennings 2017), is classically expected to lead to faster evolution (Barrett and Schluter 2008). TEs however, may defeat this prediction due to the combined effect of their stress-inducible activity and large mutagenic properties (Baduel et al. 2021). *ONSEN*, because of its insertion bias towards actively transcribed, H2A.Z-rich regions in the *A. thaliana* genome (Quadrana et al. 2019; Roquis et al. 2021) and its ability to translate heat-stress into a transcriptomic response, has recently gained attention in the context of natural adaptation (Baduel et al. 2021; Legrand et al. 2019; Quadrana et al. 2016, 2019; Ito et al. 2016). Here, we experimentally confirm with a real-time setup that a single novel insertion of *ONSEN* can indeed rapidly lead to drought-resistant individuals.

We took advantage of *ONSEN* hc-lines that originate from Col-0 plants that were heat-stressed and transiently exposed to zebularine and alpha-amanitin, two drugs known to interfere with TE-silencing (Baubec et al. 2009; Thieme et al. 2017). While this treatment has been shown to induce epi/genetic mutations (Liu et al. 2015; Roquis et al. 2021), we did not observe a general effect of these drugs on plant size compared to the wt. Yet, in line with the fact that transposition is predominantly associated with fitness loss of the host (Chuong et al. 2017; Boissinot et al. 2006; Wilke and Adams 1992; Roquis et al. 2021), several hc-lines showed a reduced size under well-watered conditions. As we also observed significant size differences between segregating hc-lines originating from the same parent, we suggest that single insertion events rather than the overall *ONSEN*-load were underlying the phenotypic variation. In contrast, we found that upon water-limitation, a reduced plant size turns to an advantage and leads to a high frequency of drought resistant hc-lines.

Among those, hc31 was fully resistant to desiccation stress and therefore further characterized. By combining genetic crosses and analysis of transcriptomic data of hc31, we were able to unequivocally attribute this effect to a novel insertion of *ONSEN* resulting in a LoF mutation of *RPI2*. In accordance with previous work (Xiong et al. 2009), the decrease of the SPAD-value (Ling et al. 2011) and the C/N-ratio (Otori et al. 2017) suggested that the inserted *ONSEN*-copy caused a reduction of the photosynthesis rate leading to decelerated growth and reduced water consumption allowing hc31 to escape severe drought stress.

Because we also found *RPI2* to be associated with aridity levels in natural *A. thaliana* populations, we further conclude that TEs can enhance the function of quantitative loci through LoF and lead to fast adaptation to fluctuating environments. In *A. thaliana*, several

studies have established a functional link between LoF and adaptive traits (e.g. Johanson et al. 2000; Gujas et al. 2012; Kroymann et al. 2003) also in the context of adaptation to drought (Monroe et al. 2018; Xu et al. 2019). Importantly, it was also found that variations in the growth scaling of natural accessions of *Arabidopsis* are linked to abiotic parameters such as temperature and precipitation (Vasseur et al. 2018). Together with this large body of evidence, our study substantiates the “less is more” hypothesis (Olson 1999) and that, in contrast to intuitive expectations, gene loss may fuel evolution.

We did not find TIPs in *RPI2* of any of the 1047 natural ecotypes of the 1001 Genomes project (Baduel et al. 2021). Because the insertion of *ONSEN* in *RPI2* leads to a reduced photosynthetic activity and smaller plant size, one may expect insertions with such fitness effects to be purged by natural selection. This mechanism would suggest a transient adaptive effect of active TEs which might be difficult to capture with population genomics data. Our simulation indeed confirms that a mutation with high deleterious effects under optimal growth conditions is hardly maintained over time (Fig S4). Yet, our simulation also shows that this mutation reaches much higher frequency when the population encounters repeated drought events, demonstrating that *ONSEN* or other heat-responsive TEs could provide a selective advantage in the face of global warming. On the other hand, positively selected LoF mutations leading to semidwarfness of *Arabidopsis* have been reported earlier (Barboza et al. 2013) and the absence of TIPs in *RPI2* could also indicate that this transposition event did not take place in the wild or only occurred in marginal populations not yet sampled. Indeed, TE-mediated mechanisms leading to large-effect mutations might be especially important in less adapted, frequently stressed populations where drastically altered phenotypes could be advantageous. In agreement with this hypothesis, Baduel et al. (2021) recently pointed towards a link between positive selection of weak *NRPE* alleles and a globally relaxed silencing of TEs in *A. thaliana* ecotypes growing under extreme conditions. Selection experiments with populations of hc-lines whose TE-composition has not yet been shaped by natural selection will allow us to extrapolate the overall gain or loss of plant fitness following a heat-induced transposition in wild populations. Altogether, we support the notion that mobilzed TEs, due to their propensity to disrupt genes and to create LoF mutations, will play an important role in adaptation to changing environments.

Material Methods

4.1 Plant material

ONSEN hc-lines were generated by the combined treatment of Col-0 plants with a heat-shock and drugs that inhibit TE-silencing as described previously (Thieme et al. 2017). Briefly, seeds of Col-0 were germinated and grown under long day conditions (16h light) at 24 °C (day) 22 °C (night) on ½ MS medium (1% sucrose, 0.5% Phytagel, pH 5.8). To reduce TE-silencing and increase the rate of *ONSEN* transposition seedlings were grown analogously on ½ MS medium supplied with sterile filtered zebularine (Z, 40 µM) and α-amanitin (A, 5 mg/ml). After seven days of growth on control ½ MS or medium supplied with A and Z, seedlings were ether exposed to control stress (CS 24 h at 6 °C followed by 24 h at normal conditions) or heat stress (HS, 24 h at 6°C followed by 24h at 37 °C), rescued onto soil and selfed to obtain the S1-generation. Individual S1 plants originating from plants that were either only exposed to CS or HS or additionally treated with A and Z (AZ) were separated and repeatedly self-fertilized until we obtained the S4 generation. In this study we used 23 *ONSEN* hc-lines originating from 13 plants that were treated with HS+AZ, five independent lines that were either only exposed to CS (two lines), HS (two lines) or CS+AZ (one line) and the Col-0 wild type that was propagated on soil. The *rpi2-1*-mutant (SALK_022117) was obtained from the NASC (Alonso et al. 2003).

4.2 qPCR for *ONSEN* copy numbers

To determine the average *ONSEN* copy numbers of the hc-lines and controls used in this study, we extracted DNA of the areal parts of pools of 50 individuals per line of the S4 generation grown for eight days under sterile conditions on ½ MS medium (1% sucrose, 0.5% Phytagel, pH 5.8) under long day condtions (16h light) at 24 °C (day) 22 °C (night) using the DNeasy Plant Kit (Qiagen). *ONSEN* copy numbers were determined by qPCR using 12 ng total DNA using the KAPA SYBR FAST master mix universal on a C1000 Touch (Bio-Rad) machine. *ACTIN2* (*At*3g18780) was used to normalize DNA-levels and DNA of Col-0 served as a control. Three technical replicates were used and data were analyzed with the Bio-Rad CFX Manager 3.1 software. Sequences of oligos are listed in Table S2.

4.2 Identification and visualization of *ONSEN* and T-DNA insertions

Novel *ONSEN*-insertions of hc31 were identified and characterized recently (Roquis et al. 2021) by whole genome sequencing and using the Transposable Insertion Finder v1.6 (Nakagome et al. 2014) and the TAIR10 version of the *A. thaliana* Col-0 reference genome (Berardini et al. 2015). To validate the presence and zygosity of the *ONSEN* and T-DNA-insertions in *RPI2* in the segregating F2 populations, we designed primers (mto_007 and mto_067) spanning the predicted insertion sites of *ONSEN* and the T-DNA (based on SIGnAL) and combined them with primers specific to *ONSEN* (mto_196) or the T-DNA (LBb1.3 mto_063) (Fig 3a, Table S2). For the PCRs we used a standard TAQ DNA polymerase (Sigma Aldrich) and limited the elongation time to 90 seconds so that an homozygous insertion of the 5 kb *ONSEN*-TE or the T-DNA would prevent the formation of a PCR-product. For the genotyping of the F2 populations we used DNA of homozygous parental plants (wt, hc31, SALK_022117).

RNA-seq data of one representative biological replicate of the Col-0 wt and hc31 exposed to CS and whole genome sequencing data of hc31 were obtained from and analyzed according to (Roquis et al. 2021). Genomic reads were mapped to the TAIR10 version of the *Arabidopsis* genome using bwa mem (v. 0.7.17-r1188) (Li and Durbin 2009) with the -M parameter set. The insertion site of *ONSEN* was then visualized using the packages Gviz (v. 1.28.3) (Hahne and Ivanek 2016), rtracklayer (v. 1.44.4) (Lawrence et al. 2009) and the annotation package TxDb.Athaliana.BioMart.plantsmart28 (v. 3.2.2) (Carlson and Maintainer 2015) using R (v. 3.6.3) (R Core Team 2020) (R Core Team 2020) in Rstudio (v. 1.1.456) (RStudio Team 2016).

4.3 Desiccation assay

To obtain comparable and robust results, we ran one comprehensive desiccation experiment where we tested the S4 generation of hc-lines and the control lines and the segregating F2 generations of a cross of the hc31 and Col-0 and hc31 and SALK_022117 in parallel. We included five replicates for each hc- and control line and of the parents of the cross between SALK_022117 and hc31 and tested 22 F2-individuals of the cross of hc31 with the wt and 16 F2-individuals of the cross of hc31 and SALK_022117. Seeds were sown onto pots filled with Einheitserde that was incubated with 75 mg/L Kohinor (Leu+Gygax AG) and kept at 4°C for three days. After stratification, pots were moved into a Hiros climate chamber (Clitec) set to short day conditions with 10 h light (LED Valoya Ns12 C75/65, ~120umol*m-2*s-1) and 22°C (day) and 19°C (night), 60% humidity. After ten days of growth, seedlings were piqued into pots filled with equal amounts of Kohinor treated soil and grown under well-watered conditions for 36 days. Position of pots was frequently shifted to ensure similar growth

conditions. Before watering was suspended, pots were again saturated with water and weighted to obtain the maximal water content. One day later (day 1 of the experiment), top-view pictures were taken with a Canon EOS 70D camera on a tripod and the following settings: 5.6s shutter opening, 1/60 shutter speed, ISO 200. This procedure was repeated three times at an interval of seven days until day 22 of the experiment. On day 27 pots were again weighted, top-view pictures were taken and drought stress was stopped by filling trays with water and allowing the pots to soak water over night. After two days of regeneration under well-watered conditions final pictures of the plants were taken (day 29). To account for different zoom levels during the course of the experiment we took pictures of a white label that later served a calibrator to normalize predicted vital and wilted leaf areas. One day after the last pictures were taken, one leaf of each plant from the segregating F2 populations was sampled for DNA-extractions and genotyping. Pots were removed from the climate chamber and dried for 8 weeks at room temperature to obtain the dry weight that allowed us to calculated the water content of each pot. Because except for day 27 pictures and weight were determined on two successive days, we extrapolated the weight measurements to determine the water content on the exact days pictures were taken.

4.4 Machine learning based prediction of wilted and vital leaf areas

We used the pixel classification tool of ilastik (v. 1.3.3post3) (Berg et al. 2019) with all 13 features for color/intensity, edge, texture of sigma 0.3, 0.7 and 10.00 selected. We defined three different pixel classes namely “background”, “wilted” and “green”, performed an iterative manual training to gradually improve the accuracy of the prediction and finally used 24 images of plants at different stages of the experiment for the training of the model. For the disc-assay we combined one to three leaf-discs that were punched from vital and wilted leaves onto a single pot that did not contain a plant. We took three pictures of each combination. To cover a broad spectrum of possibilities, leaf discs were shuffled and/or moved on the pot between pictures. Hence some discs were photographed multiple times but in different combinations and/or positions. Analogously to the training of vital and wilted areas, we used five images to train ilastik to detect background and the white labels that served as a scale to normalize pixel counts between different days of the experiment. We then processed and exported all image files in ilastik the with following settings: source: “simple segmentation”, convert to datatype: “floating 32 bit”, format: “tif” and used the getHistogram function of ImageJ (v. 1.53g, Java 1.8) (Schneider et al. 2012) to extract the pixel counts of the areas predicted by ilastik. Pixel counts of green and wilted leaves were then normalized using the predicted areas of the size references for each time point of the desiccation experiment using R.

4.5 SPAD-value and C/N ratio

We grew plants of the S4 generation under the same conditions and watering regime as for the desiccation experiment and used a chlorophyll meter SPAD-502 (Ling et al. 2011) to determine the SPAD-values of three or six leaves of six wt and hc31 plants that were grown as triplicates in two independent experiments. SPAD-values were measured before the occurrence of drought induced wilting 15 days after watering was suspended.

To determine the carbon/nitrogen ratios of the wt and hc31 we grew plants of the S3 generation under well-watered conditions on Einheitserde under short day conditions in a Sanyo MLR-350 growth chamber with 8 h light at 20 °C (day) and 18 °C (night) for 14 weeks. We sampled each one leaf of four plants of the wt and hc31, inactivated them for 30 seconds in a microwave and dried them for eight days at 60°C. Plant material was then grinded for 3 minutes at 30 hz with an oscillating Mill (M M 400, Retsch, Germany). 2 mg of plant material were put in tin capsule and samples were analyzed by the Basel Stable Isotope Lab.

4.6. *RPI2* and natural population analysis

We used the vcf produced by The 1001 genome consortium (Alonso-Blanco et al. 2016) to extract SNPs for 1135 sequenced accessions of *A. thaliana*. To limit the effect of phylogenetic relationship in further analyses, we used the function –relatedness2 from vcftools (Danecek et al. 2011) to keep only ecotypes with a kinship coefficient k <0.05. For the remaining ecotypes, bioclimatic variables (https://www.worldclim.org/data/worldclim21.html) and Global Aridity Index (https://cgiarcsi.community/data/global-aridity-and-pet-database/) were extracted using the Rpackages raster (v. 3.5-2; Hijmans and van Etten 2012) and rgdal (v. 1.5-27; (Keitt et al. 2010). We fitted a linear-mixed model with the R package lme4 (v. 1.1-27; Bates et al. 2015) to test the association between aridity levels averaged over May to August and SNPs in *RPI2* harboring a minor allele frequency (maf) > 0.3. We added the admixture groups defined by The 1001 genome consortium (Alonso-Blanco et al. 2016) as a random effect to account for population structure. We used QGIS (v. 3.16; https://www.qgis.org/en/site/) to display *RPI2* alleles in Eurasia. For the rest of the manuscript, all statistical analyses were performed in R and used parametric or non-parametric test according to the sample size and data distribution.

4.7. Survival probability of *ONSEN* in *RPI2*

TIPs in *RPI2* were screened in the data published by Baduel et al. (2021). We used forward-in-time models to examine the short-term fate of a TE inserting in *RIP2*, simulating a population of 100 diploid individuals undergoing drought events. We used the SliM3 simulator (Haller and Messer 2019) to model a population with a selfing rate of 99% (Richard et al. 1989), and ran the simulations for 50 generations. Assuming a generation time of about two months and six months of suitable growth conditions per year, this simulation should cover approximately 16 years of a natural population. The TE insertion only had a fitness effect at the homozygous state (dominance coefficient *h*=0) and was initially sampled during the first generation from a single genome (over 200). The selective advantage (*s*) of individuals carrying the TE insertion at the homozygous state during the drought events was set at +50%, +100%, +200% or +500% relative to the wildtype. During normal conditions, this coefficient was set at -10%, -20%, -50% or -90% relative to the wildtype. We applied a model of hard selection, with a population size being a function of the average fitness, with a maximal population size of 100 (carrying capacity). This was included as a way to consider the varying effects of drift in small populations, which may affect the odds for a deleterious allele to rise in frequency. We simulated one to four drought events at regular intervals. Each of these events could last two, three, or four generations. We ran 1000 simulations for each combination of parameters. Scripts are freely available at https://github.com/YannBourgeois/Slim-simu-TE

Data availability

Image files and the ilastik trainings and raw data were uploaded to Zenodo

Supplementary data

Table S1 SNPs in *RIP2* and Bioclimatic variables for the 596 subsetted ecotypes.

Table S2 Names and sequences of oligos used for the qPCR to determine *ONSEN* copy numbers and for genotyping of *RPI2*

Acknowledgements

We would like to thank Anja Schmutz for her support with R. We further want to thank Ansgar Kahmen, Thomas Boller and Monika Messmer for their involvement at the beginning of the project.

Author contributions: experimental design: M.T. and A.B.; data acquisition: M.T., B.K. and A.B.; data analysis: M.T., A.R. and Y.B.; writing of the manuscript: M.T. with contributions from A.R.,Y.B., E.B., A.B. and B.K.

Funding

University of Zurich Research Priority Programs (URPP) *Evolution in Action* (to M.T., B.K. and A.R.);

European Commission [PITN-GA-2013-608422-IDP BRIDGES] and Freiwillige Akademische Gesellschaft Basel (to M.T.);

[SNSF 31003A_182785] (to A.R. and B.K.)

European Research Council (ERC) under the European Union's Horizon 2020 research and innovation program [725701, BUNGEE] (to E.B.);

Supplementary figures

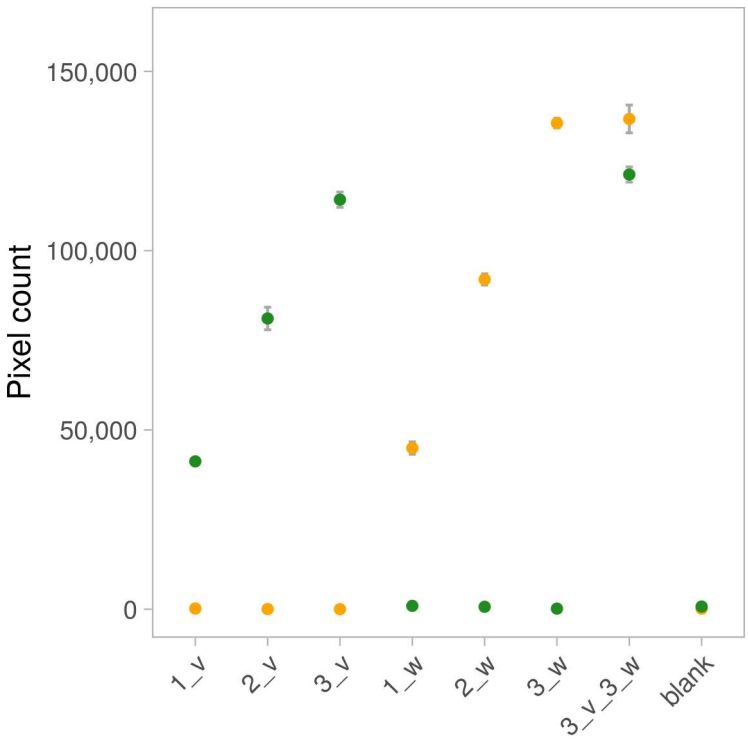

Fig S1. Leaf disc assay for the validation of the accuracy of the predicted vital (green) and wilted (yellow) pixel counts using the machine learning software ilastik. One, two or three discs were punched from vital (v) or wilted (w) leaves and placed onto an empty pot (blank). n=3 technical replicates.

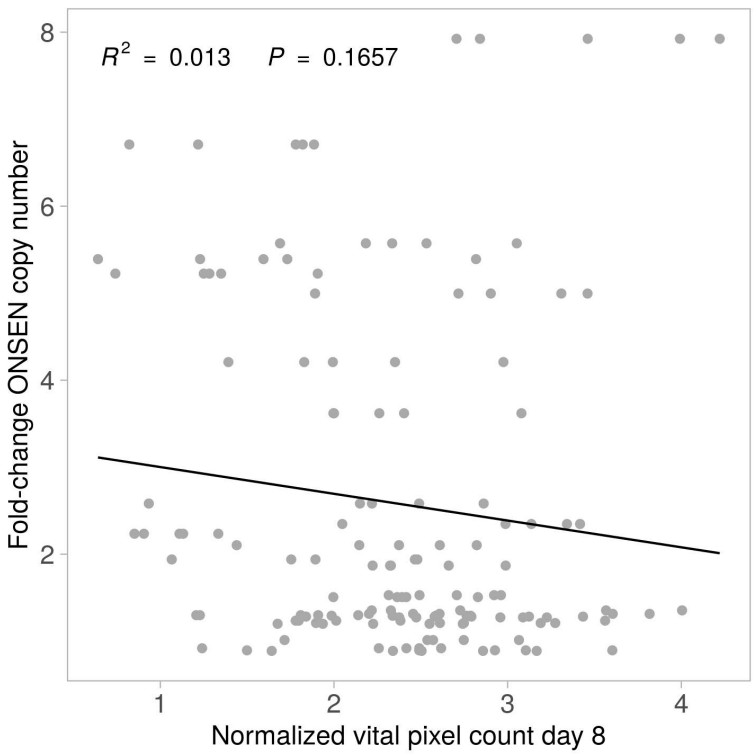

Fig S2. Vital pixel count of all tested lines before the occurrence of wilted leaves (day 9) (n=5 biological replicates) and the fold change of *ONSEN*-copy numbers measured by qPCR relative to the wt (n=3 technical replicates). Linear regression model, adjusted R-squared: 0.013, P=0.1657

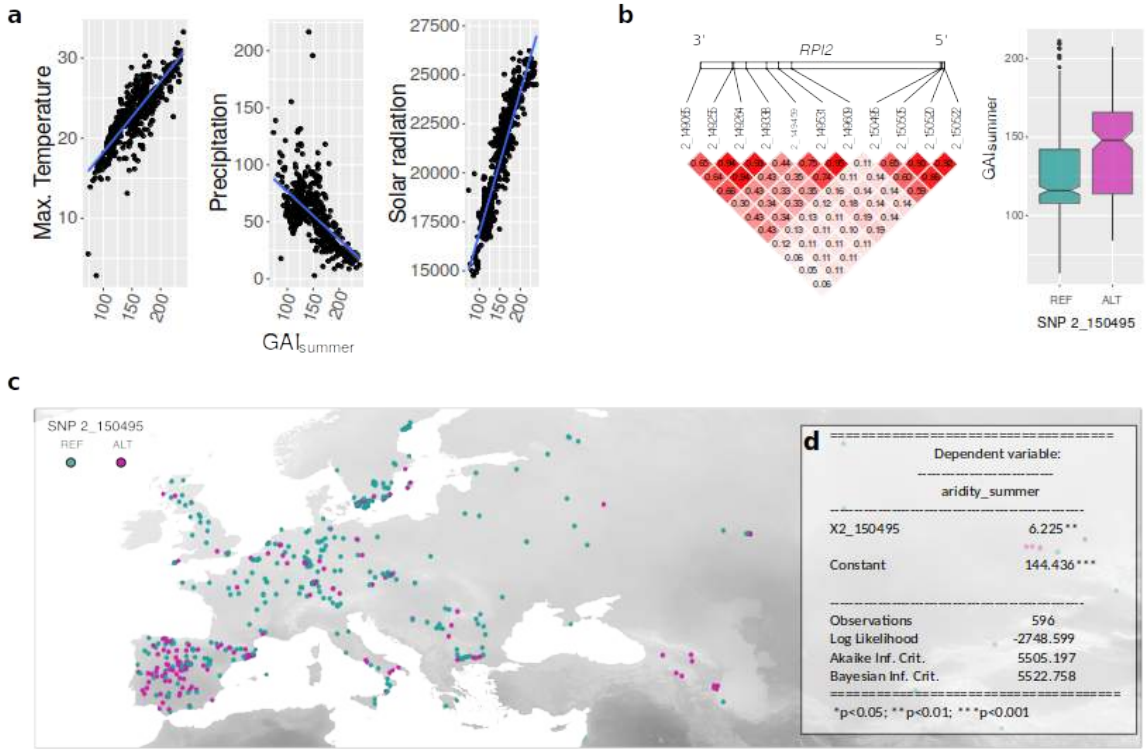

Fig S3 Aridity and *RPI2* in natural populations of *A. thaliana* **a** Correlation between GAIsummer, temperature, precipitation and solar radiation extracted for each sample site. **b** Linkage disequilibrium among the 11 SNPs located in *RPI2* (left panel) and association between SNP 2_150495 and GAIsummer (right panel). **c** Occurrence of the reference and alternative alleles of SNP 2_150495 in Eurasia. **d** Linear mixed-model results.

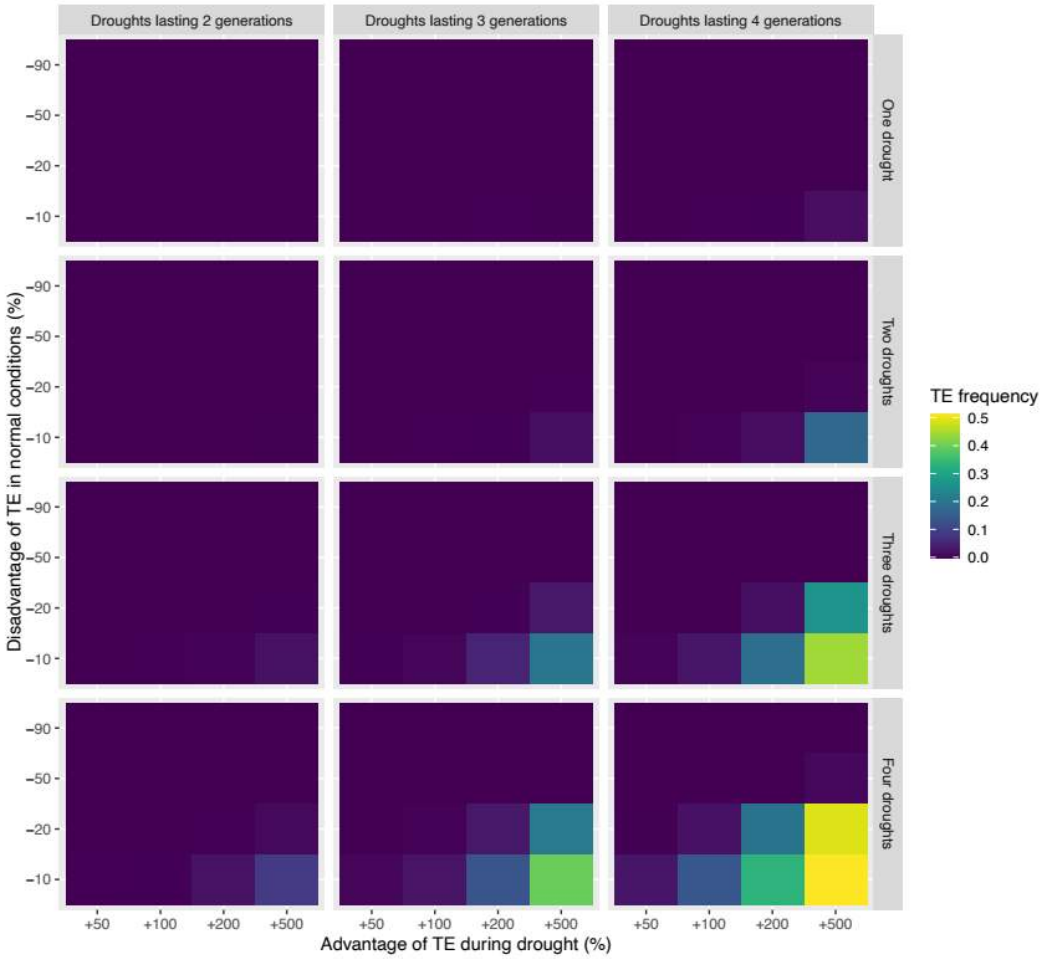

Fig S4 Simulated frequency of a TE-insertion in a population of *A. thaliana* exposed to drought stress Heatmap showing the average frequency of TE-insertions with differing fitness impacts under control and drought conditions in response to increasing intensity of drought stress after 50 generations. Each cell in the heatmap corresponds to 1000 simulations.

References

Alonso-Blanco C, Andrade J, Becker C, Bemm F, Bergelson J, Borgwardt KMM, Cao J, Chae E, Dezwaan TMM, Ding W, et al. 2016. 1,135 Genomes Reveal the Global Pattern of Polymorphism in Arabidopsis thaliana. *Cell* **166**: 481–491.

Alonso JM, Stepanova AN, Leisse TJ, Kim CJ, Chen H, Shinn P, Stevenson DK, Zimmerman J, Barajas P, Cheuk R, et al. 2003. Genome-wide insertional mutagenesis of Arabidopsis thaliana. *Science (80-)* **301**: 653–657.

Baduel P, Leduque B, Ignace A, Gy I, Gil J, Loudet O, Colot V, Quadrana L. 2021. Genetic and environmental modulation of transposition shapes the evolutionary potential of Arabidopsis thaliana. *Genome Biol* **22**: 138.

Barboza L, Effgen S, Alonso-Blanco C, Kooke R, Keurentjes JJB, Koornneef M, Alcázar R. 2013. Arabidopsis semidwarfs evolved from independent mutations in GA20ox1, ortholog to green revolution dwarf alleles in rice and barley. *Proc Natl Acad Sci U S A* **110**: 15818–15823.

Barrett RDH, Schluter D. 2008. Adaptation from standing genetic variation. *Trends Ecol Evol* **23**: 38–44.

Bates D, Mächler M, Bolker BM, Walker SC. 2015. Fitting linear mixed-effects models using lme4. *J Stat Softw* **67**: 1–48.

Baubec T, Pecinka A, Rozhon W, Mittelsten Scheid O. 2009. Effective, homogeneous and transient interference with cytosine methylation in plant genomic DNA by zebularine. *Plant J* **57**: 542–554.

Belfield EJ, Brown C, Ding ZJ, Chapman L, Luo M, Hinde E, van Es SW, Johnson S, Ning Y, Zheng SJ, et al. 2021. Thermal stress accelerates arabidopsis thaliana mutation rate. *Genome Res* **31**: 40–50.

Berardini TZ, Reiser L, Li D, Mezheritsky Y, Muller R, Strait E, Huala E. 2015. The arabidopsis information resource: Making and mining the “gold standard” annotated reference plant genome. *genesis* **53**: 474–485.

Berg S, Kutra D, Kroeger T, Straehle CN, Kausler BX, Haubold C, Schiegg M, Ales J, Beier T, Rudy M, et al. 2019. ilastik: interactive machine learning for (bio)image analysis. *Nat Methods* **16**: 1226–1232.

Boissinot S, Davis J, Entezam A, Petrov D, Furano A V. 2006. Fitness cost of LINE-1 (L1) activity in humans. *Proc Natl Acad Sci U S A* **103**: 9590–9594.

Bourgeois Y, Boissinot S. 2019. On the Population Dynamics of Junk: A Review on the Population Genomics of Transposable Elements. *Genes (Basel)* **10**.

Brás TA, Seixas J, Carvalhais N, Jagermeyr J. 2021. Severity of drought and heatwave crop losses tripled over the last five decades in Europe. *Environ Res Lett* **16**: 065012.

Butelli E, Licciardello C, Zhang Y, Liu J, Mackay S, Bailey P, Reforgiato-Recupero G, Martin C. 2012. Retrotransposons Control Fruit-Specific, Cold-Dependent Accumulation of Anthocyanins in Blood Oranges. *Plant Cell* **24**: 1242–1255.

Carlson M, Maintainer BP. 2015. TxDb.Athaliana.BioMart.plantsmart28: Annotation package for TxDb object(s).

Cavrak V V, Lettner N, Jamge S, Kosarewicz A, Bayer LM, Mittelsten Scheid O. 2014. How a retrotransposon exploits the plant’s heat stress response for its activation. *PLoS Genet* **10**: e1004115.

Chuong EB, Elde NC, Feschotte C. 2017. Regulatory activities of transposable elements: from conflicts to benefits. *Nat Rev Genet* **18**: 71–86.

Dai A. 2013. Increasing drought under global warming in observations and models. *Nat Clim Chang* **3**: 52–58.

Danecek P, Auton A, Abecasis G, Albers CA, Banks E, DePristo MA, Handsaker RE, Lunter G, Marth GT, Sherry ST, et al. 2011. The variant call format and VCFtools. *Bioinformatics* **27**: 2156–2158.

Esnault C, Lee M, Ham C, Levin HL. 2019. Transposable element insertions in fission yeast drive adaptation to environmental stress. *Genome Res* **29**: 85–95.

Exposito-Alonso M, Gómez Rodríguez R, Barragán C, Capovilla G, Chae E, Devos J, Dogan ES, Friedemann C, Gross C, Lang P, et al. 2019. Natural selection on the Arabidopsis thaliana genome in present and future climates. *Nature* **573**: 126–129.

FAO. 2019. *PROACTIVE APPROACHES TO DROUGHT PREPAREDNESS Where are we now and where do we go from here? Where are we now and where do we go from here?*

Grandbastien MA. 2015. LTR retrotransposons, handy hitchhikers of plant regulation and stress response. *Biochim Biophys Acta* **1849**: 403–416.

Gujas B, Alonso-Blanco C, Hardtke CS. 2012. Natural arabidopsis brx loss-of-function alleles confer root adaptation to acidic soil. *Curr Biol* **22**: 1962–1968.

Gupta A, Rico-Medina A, Caño-Delgado AI. 2020. The physiology of plant responses to drought. *Science (80-)* **368**: 266–269.

Hahne F, Ivanek R. 2016. Visualizing genomic data using Gviz and bioconductor. In *Methods in Molecular Biology*, Vol. 1418 of, pp. 335–351, Humana Press Inc.

Haller BC, Messer PW. 2019. SLiM 3: Forward Genetic Simulations Beyond the Wright–Fisher Model ed. R. Hernandez. *Mol Biol Evol* **36**: 632–637.

Hermisson J, Pennings PS. 2017. Soft sweeps and beyond: understanding the patterns and probabilities of selection footprints under rapid adaptation ed. J. Kelley. *Methods Ecol Evol* **8**: 700–716.

Hijmans RJ, van Etten J. 2012. raster: Geographic analysis and modeling with raster data.

Ito H, Gaubert H, Bucher E, Mirouze M, Vaillant I, Paszkowski J. 2011. An siRNA pathway prevents transgenerational retrotransposition in plants subjected to stress. *Nature* **472**: 115–119.

Ito H, Kim J-M, Matsunaga W, Saze H, Matsui A, Endo TA, Harukawa Y, Takagi H, Yaegashi H, Masuta Y, et al. 2016. A Stress-Activated Transposon in Arabidopsis Induces Transgenerational Abscisic Acid Insensitivity OPEN. *Nat Publ Gr*.

Johanson U, West J, Lister C, Michaels S, Amasino R, Dean C. 2000. Molecular analysis of FRIGIDA, a major determinant of natural variation in Arabidopsis flowering time. *Science (80-)* **290**: 344–347.

Keitt TH, Bivand R, Pebesma E, Rowlingson B. 2010. rgdal: Bindings for the “Geospatial” Data Abstraction Library.

Kroymann J, Donnerhacke S, Schnabelrauch D, Mitchell-Olds T. 2003. Evolutionary dynamics of an Arabidopsis insect resistance quantitative trait locus. *Proc Natl Acad Sci U S A* **100**: 14587–14592.

Lawrence M, Gentleman R, Carey V. 2009. rtracklayer: An R package for interfacing with genome browsers. *Bioinformatics* **25**: 1841–1842.

Legrand S, Caron T, Maumus F, Schvartzman S, Quadrana L, Durand E, Gallina S, Pauwels M, Mazoyer C, Huyghe L, et al. 2019. Differential retention of transposable element-derived sequences in outcrossing Arabidopsis genomes. *Mob DNA* **10**: 30.

Li H, Durbin R. 2009. Fast and accurate short read alignment with Burrows-Wheeler transform. *Bioinformatics* **25**: 1754–1760.

Li Z-W, Hou X-H, Chen J-F, Xu Y-C, Wu Q, González J, Guo Y-L. 2018. Transposable Elements Contribute to the Adaptation of Arabidopsis thaliana ed. Y. Van De Peer. *Genome Biol Evol* **10**: 2140–2150.

Ling Q, Huang W, Jarvis P. 2011. Use of a SPAD-502 meter to measure leaf chlorophyll concentration in Arabidopsis thaliana. *Photosynth Res* **107**: 209–214.

Lisch D. 2013. How important are transposons for plant evolution? *Nat Rev Genet* **14**: 49–61.

Liu CH, Finke A, Diaz M, Rozhon W, Poppenberger B, Baubec T, Pecinka A. 2015. Repair of DNA Damage Induced by the Cytidine Analog Zebularine Requires ATR and ATM in Arabidopsis. *Plant Cell* **27**: 1788–1800.

Loarie SR, Duffy PB, Hamilton H, Asner GP, Field CB, Ackerly DD. 2009. The velocity of climate change. *Nature* **462**: 1052–1055.

Lu Z, Cui J, Wang L, Teng N, Zhang S, Lam HM, Zhu Y, Xiao S, Ke W, Lin J, et al. 2021. Genome-wide DNA mutations in Arabidopsis plants after multigenerational exposure to high temperatures. *Genome Biol* **22**: 160.

Makarevitch I, Waters AJ, West PT, Stitzer M, Hirsch CN, Ross-Ibarra J, Springer NM. 2015. Transposable elements contribute to activation of maize genes in response to abiotic stress. *PLoS Genet* **11**: e1004915.

Matzke MA, Mosher RA. 2014. RNA-directed DNA methylation: an epigenetic pathway of increasing complexity. *Nat Rev Genet* **15**: 394–408.

Monroe JG, Powell T, Price N, Mullen JL, Howard A, Evans K, Lovell JT, McKay JK. 2018. Drought adaptation in arabidopsis thaliana by extensive genetic loss-of-function. *Elife* **7**.

Naito K, Zhang F, Tsukiyama T, Saito H, Hancock CN, Richardson AO, Okumoto Y, Tanisaka T, Wessler SR. 2009. Unexpected consequences of a sudden and massive transposon amplification on rice gene expression. *Nature* **461**: 1130–1134.

Nakagome M, Solovieva E, Takahashi A, Yasue H, Hirochika H, Miyao A. 2014. Transposon Insertion Finder (TIF): A novel program for detection of de novo transpositions of transposable elements. *BMC Bioinformatics* **15**: 71.

Negi P, Rai AN, Suprasanna P. 2016. Moving through the stressed genome: Emerging regulatory roles for transposons in plant stress response. *Front Plant Sci* **7**: 1448.

Olson M V. 1999. *MOLECULAR EVOLUTION '99 When Less Is More: Gene Loss as an Engine of Evolutionary Change*.

Otori K, Tanabe N, Maruyama T, Sato S, Yanagisawa S, Tamoi M, Shigeoka S. 2017. Enhanced photosynthetic capacity increases nitrogen metabolism through the coordinated regulation of carbon and nitrogen assimilation in Arabidopsis thaliana. *J Plant Res* **130**: 909–927.

Piegu B, Guyot R, Picault N, Roulin A, Sanyal A, Kim H, Collura K, Brar DS, Jackson S, Wing RA, et al. 2006. Doubling genome size without polyploidization: dynamics of retrotransposition-driven genomic expansions in Oryza australiensis, a wild relative of rice. *Genome Res* **16**: 1262–1269.

Quadrana L, Etcheverry M, Gilly A, Caillieux E, Madoui MA, Guy J, Bortolini Silveira A, Engelen S, Baillet V, Wincker P, et al. 2019. Transposition favors the generation of large effect mutations that may facilitate rapid adaption. *Nat Commun* **10**: 1–10.

Quadrana L, Silveira AB, Mayhew GF, Leblanc C, Martienssen RA, Jeddeloh JA, Colot V. 2016. The Arabidopsis thaliana mobilome and its impact at the species level.

R Core Team. 2020. R: A Language and Environment for Statistical Computing.

Ram H, Soni P, Salvi P, Gandass N, Sharma A, Kaur A, Sharma TR. 2019. Insertional Mutagenesis Approaches and Their Use in Rice for Functional Genomics. *Plants* **8**: 310.

Richard H, Abbott J, Gomes MF. 1989. *Population genetic structure and outcrossing rate of Arabidopsis thaliana*.

Roquis D, Robertson M, Yu L, Thieme M, Julkowska M, Bucher E. 2021. Genomic impact of stress-induced transposable element mobility in Arabidopsis. *Nucleic Acids Res*.

RStudio Team. 2016. RStudio: Integrated Development Environment for R.

Schneider CA, Rasband WS, Eliceiri KW. 2012. NIH Image to ImageJ: 25 years of image analysis. *Nat Methods* **9**: 671–675.

Stritt C, Gordon SP, Wicker T, Vogel JP, Roulin AC. 2018. Recent Activity in Expanding Populations and Purifying Selection Have Shaped Transposable Element Landscapes across Natural Accessions of the Mediterranean Grass Brachypodium distachyon. *Genome Biol Evol* **10**: 304–318.

Tenaillon MI, Hollister JD, Gaut BS. 2010. A triptych of the evolution of plant transposable elements. *Trends Plant Sci* **15**: 471–478.

Thieme M, Lanciano S, Balzergue S, Daccord N, Mirouze M, Bucher E. 2017. Inhibition of RNA polymerase II allows controlled mobilisation of retrotransposons for plant breeding. *Genome Biol* **18**: 134.

Tittel-Elmer M, Bucher E, Broger L, Mathieu O, Paszkowski J, Vaillant I. 2010. Stress-induced activation of heterochromatic transcription. *PLoS Genet* **6**: e1001175.

Vasseur F, Exposito-Alonso M, Ayala-Garay OJ, Wang G, Enquist BJ, Vile D, Violle C, Weigel D. 2018. Adaptive diversification of growth allometry in the plant Arabidopsis thaliana. *Proc Natl Acad Sci U S A* **115**: 3416–3421.

Weng M-L, Becker C, Hildebrandt J, Neumann M, Rutter MT, Shaw RG, Weigel D, Fenster CB. 2019. Fine-Grained Analysis of Spontaneous Mutation Spectrum and Frequency in Arabidopsis thaliana.

Wilke CM, Adams J. 1992. Fitness effects of Ty transposition in Saccharomyces cerevisiae. *Genetics* **131**: 31–42.

Xiong Y, Defraia C, Williams D, Zhang X, Mou Z. 2009. Deficiency in a cytosolic ribose-5-phosphate isomerase causes chloroplast dysfunction, late flowering and premature cell death in Arabidopsis. *Physiol Plant* **137**: 249–263.

Xu Y-C, Niu X-M, Li X-X, He W, Chen J-F, Zou Y-P, Wu Q, Zhang YE, Busch W, Guo Y-L. 2019. Adaptation and Phenotypic Diversification in Arabidopsis through Loss-of-Function Mutations in Protein-Coding Genes. *Plant Cell* **31**: 1012–1025.